AD NUMBER

AD888871

LIMITATION CHANGES

TO:

Approved for public release; distribution is unlimited.

FROM:

Distribution authorized to U.S. Gov't. agencies only; Test and Evaluation; 14 APR 1971. Other requests shall be referred to Air Force Avionics Laboratory, Wright-Ptterson AFB, OH.

AUTHORITY

AFAL per ltr, 5 Nov 1973

AFAL-TR-71-109

TECHNIQUES OF GAS LASER CONSTRUCTION AND PROCESSING

JAMES D. EVANS, 1st LT, USAF
WILLIAM C. EPPERS, JR.

TECHNICAL REPORT AFAL-TR-71-109

JULY 1971

AIR FORCE AVIONICS LABORATORY
AIR FORCE SYSTEMS COMMAND
WRIGHT-PATTERSON AIR FORCE BASE, OHIO

NOTICE

When Government drawings, specifications, or other data are used for any purpose other than in connection with a definitely related Government procurement operation, the United States Government thereby incurs no responsibility nor any obligation whatsoever; and the fact that the government may have formulated, furnished, or in any way supplied the said drawings, specifications, or other data, is not to be regarded by implication or otherwise as in any manner licensing the holder or any other person or corporation, or conveying any rights or permission to manufacture, use, or sell any patented invention that may in any way be related thereto.

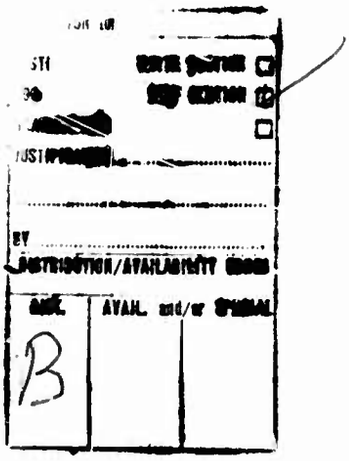

Copies of this report should not be returned unless return is required by security considerations, contractual obligations, or notice on a specific document.

AIR FORCE: 30-9-71/100

AFAL-TR-71-109

TECHNIQUES OF GAS LASER CONSTRUCTION AND PROCESSING

JAMES D. EVANS, 1st LT, USAF
WILLIAM C. EPPERS, JR.

FOREWORD

The material contained in this technical report was presented on 24 September 1970 at the IEEE 1970 Conference on Electron Device Techniques by James D. Evans, 1st Lt, USAF, of the Laser Technology Branch, Electronic Technology Division, Air Force Avionics Laboratory. Work was accomplished under Project 5237.

This report was submitted by the authors 9 April 1971.

This technical report has been reviewed and is approved for publication.

Bernard H. List

BERNARD H. LIST
Chief Scientist
Air Force Avionics Laboratory

ABSTRACT

The information presented here covers various aspects of gas laser construction and processing, in particular, the most common gas lasers: He-Ne, Noble gas-ion, CO_2, and He-Cd. In addition, some background information is given involving the theory of operation as well as the role that some of the gases play in the lasing process. An in-depth discussion of cold cathodes for the He-Ne lasers, the anodic bore ion lasers, and the CO_2 laser is included.

The material presented here is by no means all that can be reported concerning gas laser construction and processing; on the contrary, the intent here is to merely familiarize the reader with some of the problems encountered in gas laser construction and processing.

TABLE OF CONTENTS

SECTION I

INTRODUCTION

The processing methods used in constructing individual laser components determine the final operating characteristics of the laser. When processing plasma tubes, the cleaning and baking techniques are of the utmost importance. The difference between a carefully processed cathode and a hastily processed one may mean 10,000 hours in total cathode lifetime. This technical report should furnish the reader with some basic information concerning the processing and construction of gas lasers.

SECTION II

PLASMA TUBES

Figure 1 depicts a typical DC excited gas-ion laser tube (Reference 1). This tube is constructed of fused silica and is water-cooled. The bore and water jacket are usually constructed as a unit and can be used for either the induction ring discharge or the DC arc tube.

It should be pointed out that the anode and cathode are not directly on the bore axis; placing these electrodes on the bore axis tends to contaminate the window through evaporation or sputtering processes.

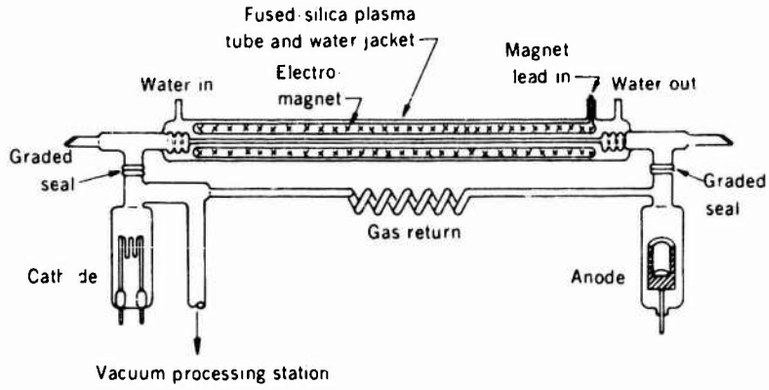

Figure 1. Typical DC-Excited Gas-Ion Laser Tube (Reproduced from Reference 1).

Figure 2 shows the radio-frequency excited CW gas-ion laser plasma tube (Reference 1). Again, this plasma tube is constructed of fused silica and is water-cooled. With the exception of graded seals and the absence of a cathode and an anode, this RF-excited ion laser tube is identical to DC arc laser tubes. The absence of metal electrodes makes the tube very tolerant of impurities and capable of CW laser action with reactive gases such as chlorine.

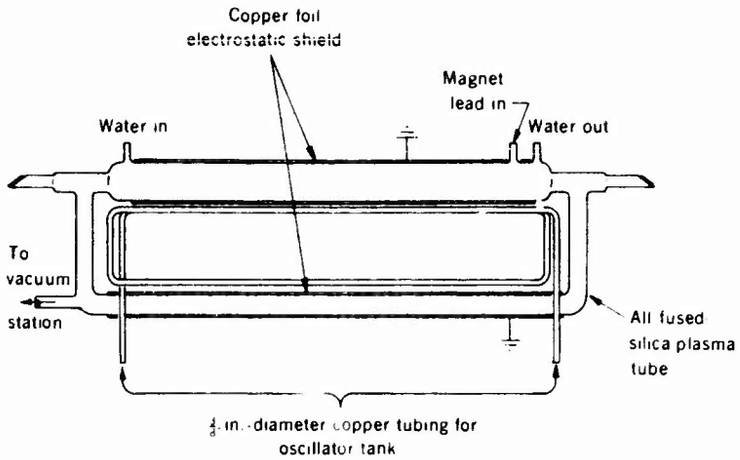

Figure 2. RF Excited CW Gas-Ion Laser Plasma Tube (Reproduced from Reference 1).

Figure 3 depicts a hollow-cathode mercury-ion laser tube (Reference 1). This tube is constructed of thin-walled metal-Kovar tubing and Kovar sealing glass. The ends of the metal tubing are flared slightly to ensure a full aperture after the glassing. In general, the most important aspect of plasma-tube assembly is to develop a procedure which will yield minimum contamination of the Brewster Windows.

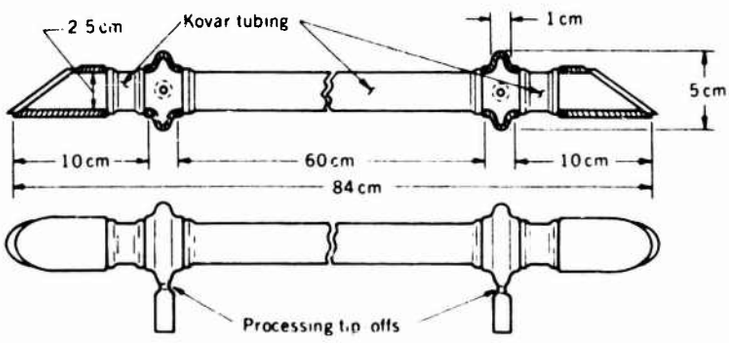

Figure 3. Hollow Cathode Mercury-Ion Laser Tube (Reproduced from Reference 1).

SECTION III

METAL VAPOR LASERS

Figure 4 shows a He-Cd laser configuration (Reference 2) which operates on the principle of cataphoresis. Since cataphoresis is proportional to ion current and back diffusion is proportional to tube diameter, one may choose a diameter small enough such that the cataphoresis effect will be dominant. Then the cataphoresis process resulting from heating the cadmium near the anode end of the tube will cause a cadmium concentration gradient sufficient for lasing. Finally, the cadmium will condense on the cold glass near the cathode.

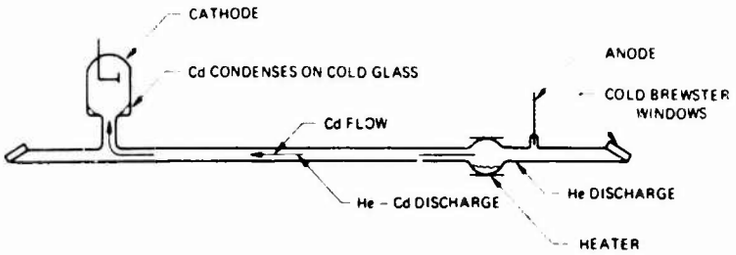

Figure 4. He-Cd Laser (Reproduced from Reference 2).

The transverse-discharge slotted hollow-cathode He-Cd laser is shown in Figure 5 (Reference 3). The slotted hollow-cathode configuration, designed by Schuebel of the Air Force Avionics Laboratory, has two main functions: it provides a discharge path that is transverse to the anode-cathode axis; and it permits metal vapors to diffuse from the space between the electrodes, into the slot in the hollow cathode. By introducing He and Cd into the laser tube at temperatures of 240°C and 360°C, six new laser lines in the region from 5337Å to 7284Å were found.

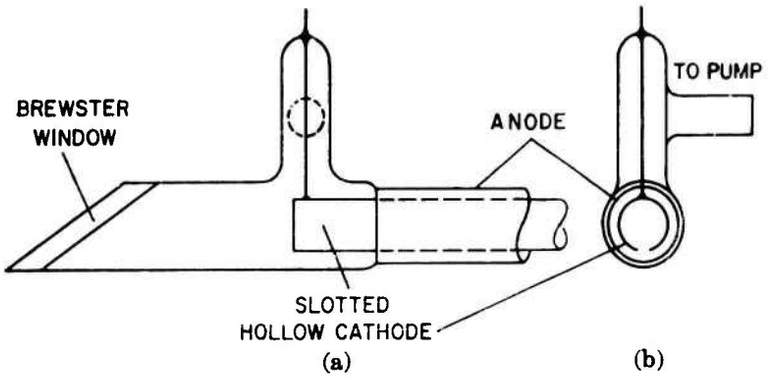

Figure 5. Transverse-discharge slotted hollow-cathode He-Cd laser (Reproduced from Reference 3).

SECTION IV

CATHODES

Figure 6 illustrates a typical multifold cathode structure which is similar in design to the first of the large area cathodes (Reference 4). This cathode is made of nickel screen, 60 x 60 mesh, of "active" #220 nickel wire, 5 mm wide and 11 cm long. It was degreased and bombarded with dry diatomic hydrogen for 30 minutes at 1000°C. The screen was then sprayed with a standard barium strontium carbonate ($BaSrCO_3$) mixture in nitrocellulose binder and formed into a multifold shape as shown. The binder was removed by air firing and the cathode mounted in a quartz tube having the dimensions of one type of argon laser as shown in Figure 7. This tube has a 2 mm bore and is 40 cm long. On the pumps, the tube was slowly heated to 250°C by tape heaters. After bakeout, the cathode was heated to 900°C in 45 minutes.

The pressure in the system did not exceed 5×10^{-5} torr during this time. The temperature was held at 900°C for 15 minutes at a pressure of 3×10^{-6} torr. The temperature was increased to 950°C for 5 minutes and then lowered to 850°C at an argon pressure of 1.0 torr for the initial emission tests. With a 100-ohm ballast resistor in the circuit, the discharge (started with the aid of a Tesla coil) was sustained at 1 ampere with a 320 volt drop for about 5 minutes. The tube was pumped and filled four times - each time drawing a higher current until the fill gas became contaminated. After five refills, the data shown in Figure 8 were obtained. The coated area of this cathode was about 10 cm^2, so the current density at 330 volts is about 1.0 A/cm^2; at 850°C this density is fair but not unusual for an oxide cathode. Following this complicated baking process, the multifold cathode was able to withstand 80 hours of operation at 10 amperes.

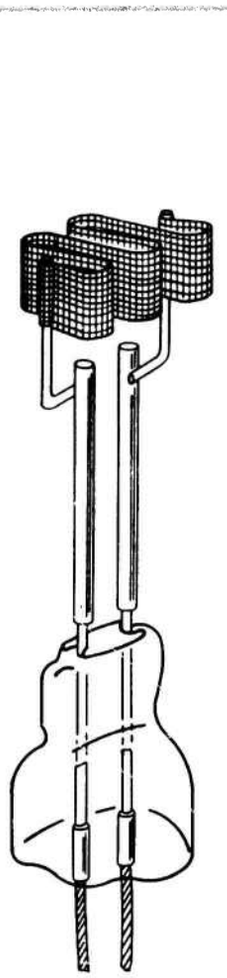

Figure 6. Multifold Cathode Structure (Reproduced from Reference 4).

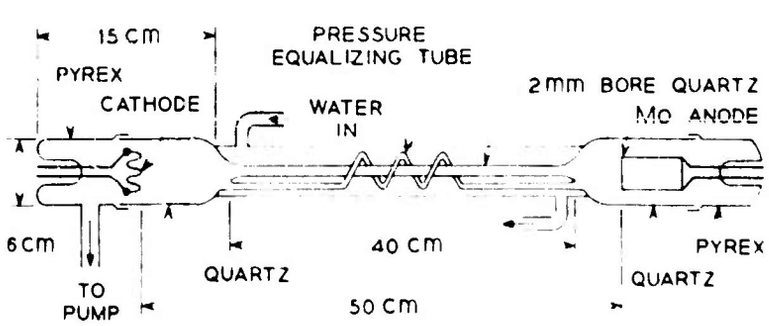

Figure 7. Cathode Tester (Reproduced from Reference 4).

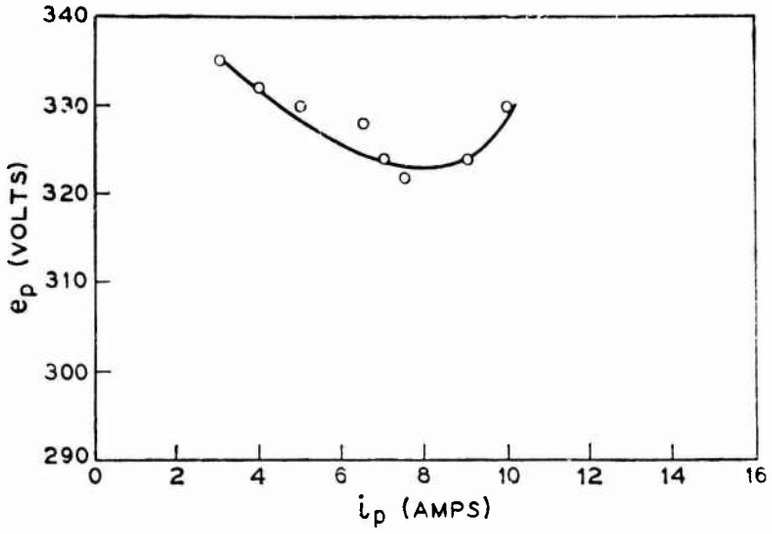

Figure 8. Current Voltage Characteristics BaSrO on Ni Screen (Reproduced from Reference 4).

Figure 9 is a diagram of a molded cathode (Reference 4). The shape of this molded cathode is just one of the many that can exist; cups, concave disks, and many other shapes can also be formed. This cathode is formed by mixing nickel powder, activators, and carbonates together, pressing this mixture into a steel die, and sintering at 1000°C.

A molded cathode such as this has several advantages, such as it suffers less from ion bombardment, and is less susceptible to poisons generated within the tube structure. Because of its low susceptibility to ion bombardment, it would be ideal for use in ion lasers such as the argon ion laser.

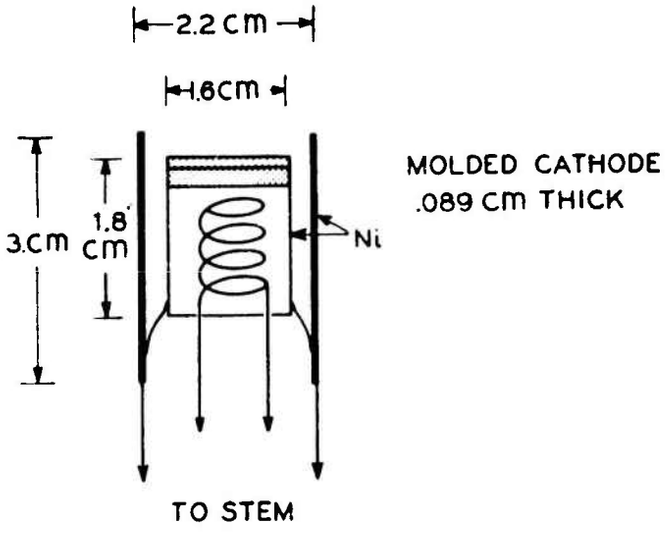

Figure 9. Molded Cathode (Reproduced from Reference 4).

SECTION V

COLD CATHODES FOR He-Ne GAS LASERS

Lifetimes of 18,000 hours have been reported by Hochuli (Reference 5) for He-Ne lasers each operating with aluminum cold cathodes at a current of 5 mA, an initial pressure of about 3 torr, and a gas volume of 42 cm^3. Properly constructed aluminum cold cathodes are responsible for this enhanced lifetime for He-Ne lasers. Cathodes made of aluminum alloy 2024 T 351 were machined in distilled water and encased in Pyrex envelopes. Outgassing and the formation of an oxide layer were achieved by ion bombardment in air or oxygen at a pressure of about 2 torr with a current density of 5 - 10 mA/cm^2 of active cathode surface.

In some cases, the pressure P (at optimum output power) vs. time curve can be approximated by the equation:

$$\frac{P}{P_0} = \left(1 - \frac{t}{\tau}\right)^{1/x} \qquad 0 \leq t \leq \tau$$

where P_0 is the initial pressure yielding optimum power output, and τ is the total lifetime of the gas discharge tube (Figure 10). If the pressure is adjusted to a new initial value P_{o_2}, the new lifetime follows the relationship:

$$\frac{\tau_2}{\tau_1} = \left(\frac{P_{o_2}}{P_{o_1}}\right)^X$$

The quantities X and τ are experimentally determined constants that depend on many variables, (current density, manufacturing process used, etc.) The lifetime τ depends on pressure, gas volume, current density, and the particular gas used.

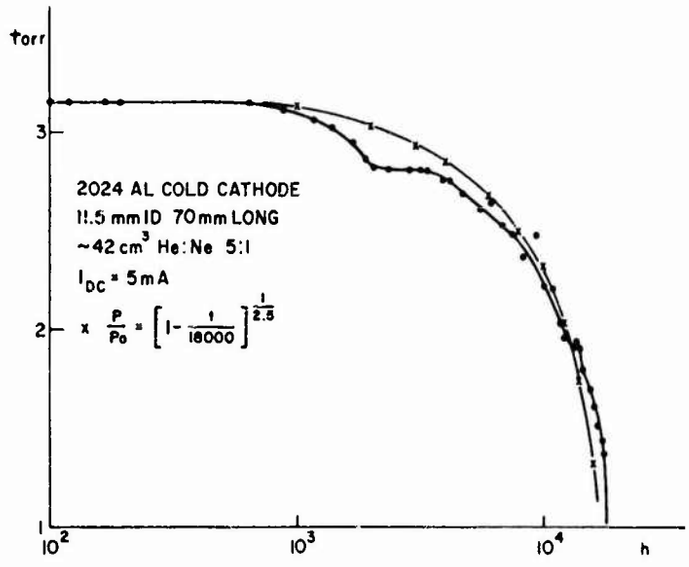

Figure 10. Pressure vs Time Curve (Reproduced from Reference 5).

SECTION VI

He-Ne GAS LASERS

Figure 11 is a cross sectional view of a space-qualified He-Ne laser proposed by Hughes Aircraft Company (Reference 6). The outstanding features of this design are:

a. Rugged all-metal-ceramic construction, allowing high-temperature bakeout and precision manufacture.

b. Long-life cold-cathode discharge, permitting highest operating efficiency and minimum heat generation.

c. Internal mirrors, reducing optical cavity losses and simplifying dust-sealing requirements while maintaining a polarized output.

d. Optimized optical cavity support structure, using materials and geometry to minimize the effects of thermal gradients, vibration, and external mechanical stresses.

e. Integrated tube and power supply package sealed with a helium atmosphere minimizing altitude-induced stresses on the optical cavity support structure, promoting cooling, and minimizing corona problems.

f. All solid-state dual power supply with precision current regulation and space-proven circuitry.

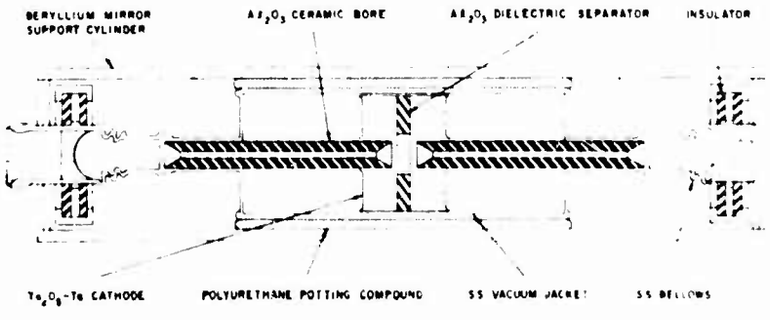

Figure 11. Space-Qualified He-Ne Laser (Reproduced from Reference 6).

Figure 12 illustrates the results obtained from experiments carried out by Suzukei (Reference 7). This graph reveals that the generation of noise depends strongly upon the discharge current and the capillary length. In general, noise is not generated at relatively small discharge currents. As the discharge current is increased slightly, an oscillation noise is generated. When the discharge current is further increased, a random noise takes the place of the oscillation noise. The critical current at which the noise appears decreases with capillary length; and the amplitude of the noise increases with capillary length. The discharge current and the capillary length must be above certain values for the noise to be generated.

The graph shows that noise problems may arise even with short length He-Ne lasers.

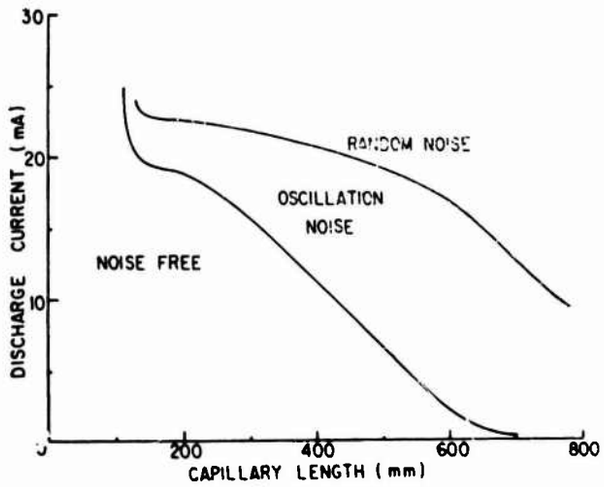

Figure 12. Criterion of the Noise Generation (Reproduced from Reference 7).

SECTION VII

ARGON ION LASERS

Figure 13 shows the electrical components of an anodic bore plasma tube (Reference 8). The primary discharge current is sustained by the plasma in contact with the conventional anode and cathode. The solenoid, which has a function similar to that in a conventional ion laser, acts to confine the plasma.

The secondary anode of the anodic bore plasma tube has a finite resistance and when the potential is applied at the anode end of the secondary anode (AESA), a modified plasma sheath is formed where the secondary anode comes into contact with the plasma. The modified plasma sheath has a potential fall of about 10 volts and acts to repel positive ions from the walls. The anodic bore plasma tube is constructed with a fused silica vacuum jacket of a conventional type. The precision bore tube contains the secondary anode, which is made from pyrolytic graphite with a metal electrode on each end.

AESA - Anode end of Secondary Anode
CESA - Cathode end of Secondary Anode

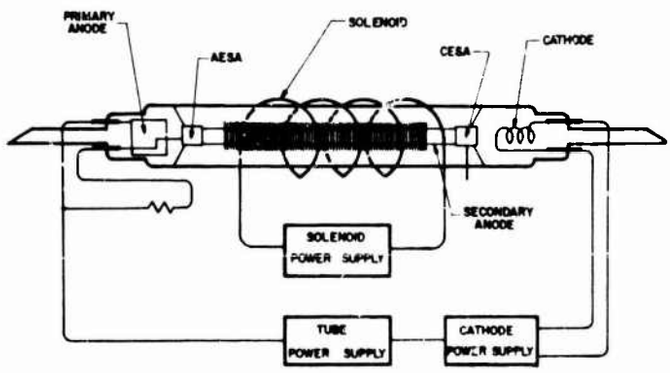

Figure 13. Electrical Components of Anodic Bore Plasma Tube (Reproduced from Reference 8).

Figure 14 is a cross sectional photograph of a piece of the actual anodic bore material (Reference 8). It was found that as the discharge current flowed from cathode to anode, positive argon ions would flow the reverse direction and would push the argon ions to one end of the bore, thus giving rise to a pressure gradient. The 4 outer bores permit the argon gas to recycle itself through the anodic bore, which eliminates the pressure gradient. The graphite cylinder is less than one inch in length and has an internal diameter of roughly 4 mm.

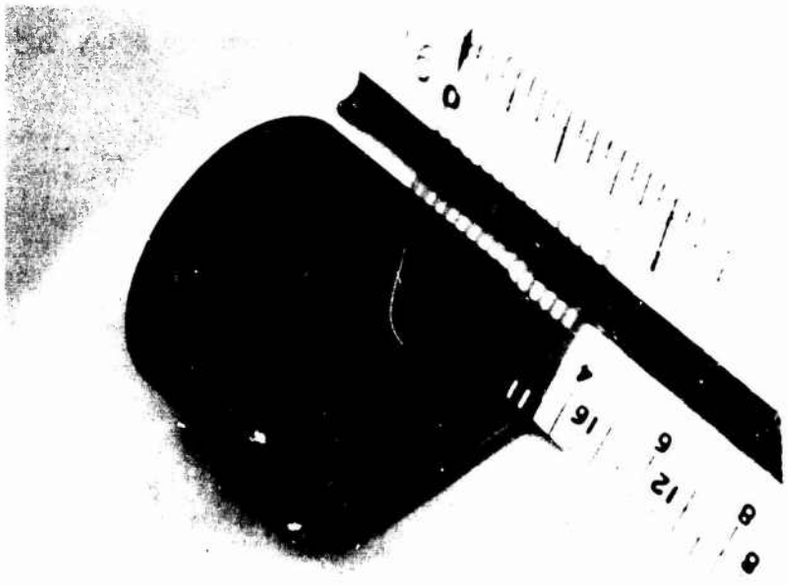

Figure 14. Cross Sectional Photograph of Anodic Bore Material (Reproduced from Reference 8).

In the past, optical degradation of the Brewster Windows has caused power limitations of high-power argon lasers. Sinclair has pointed out key problems associated with Brewster Window gas lasers, as quoted below (from Reference 14):

"The three important practical sources of optical loss in Brewster Windows are scattering, stress induced birefringence, and absorptic "

The primary cause of scattering loss in Brewster Windows is poor optical polish or scratches due to mishandling of the optically polished surfaces.

Surface films deposited on Brewster Windows exposed to the atmosphere usually increase scattering loss, but the primary effect of such films is usually absorptive loss.

Improper mounting of the Brewster Window can produce stresses which give rise to birefringence. Unless the principal axes of both windows are in the plane defined by the normals to the windows, stress-induced birefringence will cause the light in the laser cavity to become elliptically polarized. Elliptically polarized light is partially reflected by a Brewster Window; thus, stress-induced birefringence will create an optical loss in the laser cavity.

In practical laser systems, the loss caused by stress-induced birefringence can be appreciable. It tends to be particularly severe when windows are sealed to plasma tubes by direct fusion, although it has also been observed when "hard" epoxies are used to seal the windows. Loss due to stress-induced birefringence is usually very dependent on the temperature of the windows, since the forces required to create noticeable birefringence are small.

Absorptive loss can be caused either by bulk absorption in the window material or by absorption of surface films which form on the windows. The origin of surface films which cause absorptive loss (and scatter) is not always apparent. Residual films will remain on Brewster Windows if they are not adequately cleaned prior to assembly of the plasma tube; windows which are exposed to open air will, in the course of time, develop films from normal atmospheric contaminants. Films are often created by the outgassing of organic materials in the vicinity of the window; some epoxies give rise to such outgassing. Sometimes films are formed on the inside of Brewster Windows due to vapors formed by the decomposition of electrodes or the erosion of the plasma tube by the discharge.

Thermal focusing effects occur in Brewster Windows because of the temperature sensitivity of the refractive index of the window material.

When power is absorbed from the intracavity beam by the window, a refractive index gradient builds up which causes the window to display lens effects.

Figure 15 shows the setup used by Horrigan, de-Mars, and Seiden (Reference 9) to study the problem. Interferograms were made by reflecting a He-Ne laser beam directly off the Brewster Window of the high-power argon ion laser, before and during operation of the argon laser. The interferograms obtained show the thermal deformation of the Brewster Window.

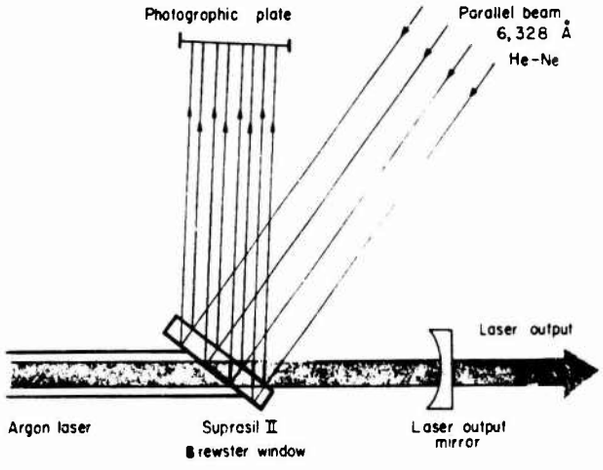

Figure 15. Setup for Obtaining Shearing Interferograms (Reproduced from Reference 9).

The three interferograms in Figure 16 were formed by the reflected light from both sides of the Brewster Window. The interferogram in (a) was made with the laser turned off and indicates no thermal deformation. The interferograms in (b) and (c) show the thermal distortion of the Brewster Window after 4 minutes of operation and 35 minutes of operation, respectively. Because a Brewster Window in direct contact with the plasma begins to absorb in the laser discharge region (due to a film buildup caused by discharge erosion of electrodes), thermal deformation takes place. This deformation degrades mode quality due to a lensing effect and significantly reduces output power.

The degrading of quality of the Brewster Windows has been the biggest cause of power limitation thus far in high-power argon ion lasers.

The rate of window degradation increases at higher currents and higher power densities, and increased degradation decreases power, shrinks beam diameter, and changes mode configuration. The Brewster Window is degraded on the side in contact with the discharge and the degradation is confined to the laser discharge region.

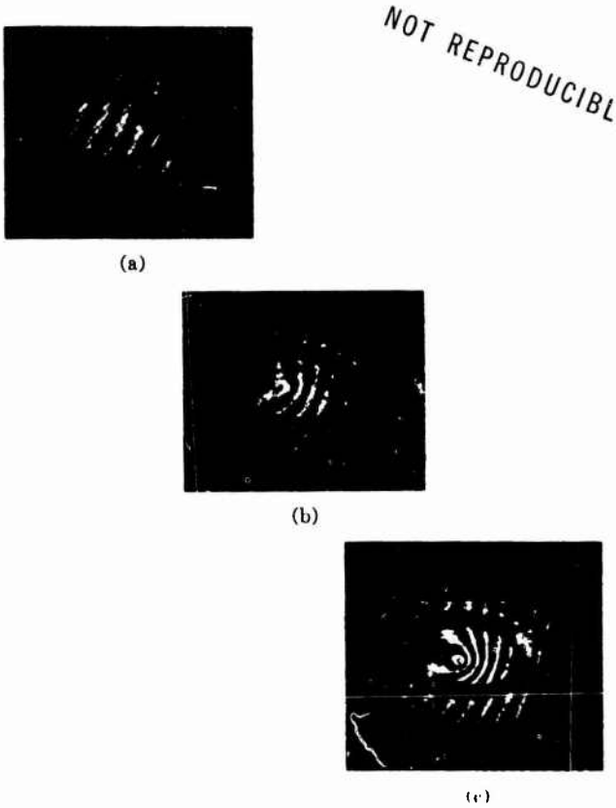

Figure 16. Interferograms Showing Optical Deformations (Reproduced from Reference 9).

SECTION VIII

HIGH POWER SINGLE MODE CO_2 LASER

Figure 17 is a diagram of a sealed-off high-power single-mode CO_2 laser that is water-cooled and has platinum electrodes (Reference 10). Electron collision and heating causes the CO_2 to dissociate into CO and O_2, which causes the concentration of CO_2 to drop and thus the power to decrease. Nitrogen is vibrationally excited at the cathode by electron impact or heating. This vibrationally excited nitrogen collides with CO_2 molecules, which produces vibrationally excited CO_2. He acts as a coolant and carries heat to the walls. The He reduces the population of the lower laser levels due to collisions.

Lifetimes of sealed-off CO_2 lasers have been short without the addition of water. Adding water improves the lifetime because when electrons impact the water, it dissociates into OH plus H. The OH then chemically combines with CO to regenerate CO_2.

In the CO_2 laser, Ni and Pt have been found to act as catalysts in regenerating CO_2. Carbone (References 11,12) has investigated the use of Ni electrodes and shown that the dominant effect is absorption of CO_2, CO, and O_2 at the Ni cathode. Another catalytic reaction was investigated by Taylor, et al (Reference 13), who observed the effects of a heated Pt wire (850°C estimated) on the output power of CO_2-He and CO_2-N_2-He mixture. Their data shows that the rate of $2CO + O_2 \rightarrow 2CO_2$ was increased by the presence of hot Pt.

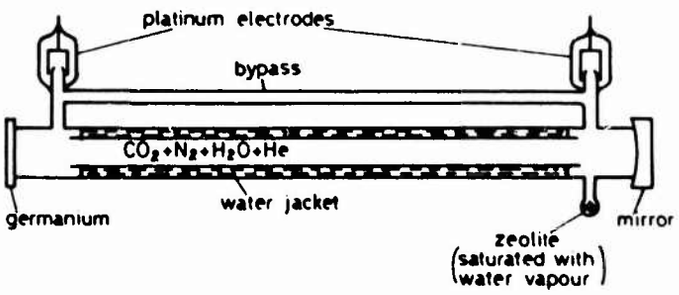

Figure 17. High Power Single Mode CO_2 Laser (Reproduced from Reference 10).

SECTION IX

CONCLUSIONS

We have indicated some of the aspects which must be considered when designing, processing, and constructing gaseous lasers. The considerations for increasing power and lifetimes include temperature of operation, cathode processing, bore design, and Brewster Window material. The He-Cd laser must operate at a high temperature, which limits the overall efficiency to a low value; operation at a low temperature is unlikely. Improved cathode processing methods are vital to improve the lifetimes of sealed gas lasers. CO_2 sealed laser lifetimes have been significantly enhanced by using platinum and nickel electrodes; these materials act as catalysts and inhibit sputtering, thereby yielding minimal tube contamination. In argon gas ion lasers, erosion of the bore has been significantly reduced by using the anodic bore; lifetimes of sealed laser tubes have been increased by a factor of ten over those for conventional plasma tubes without the anodic bore material. Brewster Windows for high-power gaseous lasers continue to present an optical problem due to physical changes in the window material; these lasers are power-limited by materials presently available for Brewster Windows. Consequently, improvements in Brewster Window materials, cathode materials and processing techniques, and bore materials and design will significantly enhance the state of the art in gas laser technology.

REFERENCES

1. Sinclair, Bell, Holt, Rinehart, Gas Laser Technology, Winston (1969) Ed.

2. Jon D. Tompkins, "He-Cd Laser," Laser Focus, August 1969.

3. Wolfgang Schuebel, "Transverse Discharge Slotted Hollow Cathode Laser," IEEE J. Quant El, Vol. QE-6, No. 9, September 1970.

4. D. McNair, "Study of Electron Emitters for Use in Gas Lasers," IEEE J. Quant El, Vol. QE-5, No. 9, September 1969.

5. U. Hochuli, "Cold Cathodes for He-Ne Gas Lasers," IEEE J. Quant El, November 1968.

6. W. B. Bridges, "Space Qualified He-Ne Laser," IEEE Conference on Laser Engineering and Applications (Digest of Technical Papers) Catalogue No. 69C27, 1969.

7. Takeo Suzuki, "A Low Noise He-Ne Laser Tube," IEEE J. Quant El, Vol. QE-5, No. 2, February 1969.

8. Willian McMahan, "Anodic-Bore Ion Laser Tube," Appl Phys Lett, Vol. 12, No. 11, June 1968.

9. de-Mars. Seiden, Horrigan, "Opitcal Degradation of High Power Ionized Argon Gas Lasers," IEEE J. Quant El, Vol. QE-4, No. 10, October 1968.

10. W. J. Witteman, "High Power Single Mode CO_2 Laser," IEEE J. of Quan El, Vol. QE-4, No. 11, November 1968.

11. Carbone, R. J., IEEE J. Quant El, QE-3, 373, 1967.

12. Carbone, R. J. IEEE J. Quant El, QE-4, 102, 1968.

13. Taylor, F. M., A. Lombardo, and W. C. Eppers, App Phys Lett, 11, 780, 1967.

14. Sinclair, D. C., "Optical Loss and Thermal Distortion in Gas Laser Brewster Windows", Applied Optics, Vol. 9, No. 4, April 1970.

 *U.S.Government Printing Office: 1971 — 759-078/126

UNCLASSIFIED

Security Classification

DOCUMENT CONTROL DATA - R & D

(Security classification of title, body of abstract and indexing annotation must be entered when the overall report is classified)

1. ORIGINATING ACTIVITY *(Corporate author)* Air Force Avionics Laboratory Wright-Patterson Air Force Base. Ohio	2a. REPORT SECURITY CLASSIFICATION UNCLASSIFIED 2b. GROUP

3. REPORT TITLE

TECHNIQUES of GAS LASER CONSTRUCTION AND PROCESSING

4. DESCRIPTIVE NOTES *(Type of report and inclusive dates)*

5. AUTHOR(S) *(First name, middle initial, last name)*

James D. Evans, 1st Lt USAF
William C. Eppers, Jr.

6. REPORT DATE	7a. TOTAL NO. OF PAGES	7b. NO. OF REFS
July 1971	29	14

8a. CONTRACT OR GRANT NO.	9a. ORIGINATOR'S REPORT NUMBER(S)
b. PROJECT NO. 5237	AFAL-TR-71-109
c.	9b. OTHER REPORT NO(S) *(Any other numbers that may be assigned this report)*
d.	

10. DISTRIBUTION STATEMENT

Distribution limited to U.S. Government agencies only; (Test and Evaluation); (statement applied 14 April 1971). Other requests for this document must be referred to AFAL/TEL, WPAFB, Ohio.

11. SUPPLEMENTARY NOTES	12. SPONSORING MILITARY ACTIVITY
	Air Force Avionics Laboratory Air Force Systems Command Wright-Patterson Air Force Base, Ohio

13. ABSTRACT

The information presented here covers various aspects of gas laser construction and processing, in particular, the most common gas lasers; He-Ne, Noble gas-ion CO_2, and He-Cd. In addition, some background information is given involving the theory of operation as well as the role that some of the gases play in the lasing process. An in-depth discussion of cold cathodes for the He-Ne lasers, the anodic bore ion lasers, and the CO_2 laser is included.

The material presented here is by no means all that can be reported concerning gas laser construction and processing; on the contrary, the intent here is to merely familiarize the reader with some of the problems encountered in gas laser construction and processing.

DD FORM 1 NOV 1473

UNCLASSIFIED

Security Classification

14. KEY WORDS	LINK A		LINK B		LINK C	
	ROLE	WT	ROLE	WT	ROLE	WT
Lasers						
He-Cd Lasers						
He-Ne Lasers						
Argon-Ion Lasers						
Cathodes						
CO_2 Lasers						
Cold Cathodes						
Cathode Processing						
Metal Vapor Lasers						
Plasma Tubes						
Brewster Windows						
Thermal Degradation						
Cataphoresis						
Slotted Hollow Cathodes						
Noise Characteristics						
Space-Qualified He-Ne Lasers						
Anodic Bores						
Optical Degradation						
Shearing Interferograms						
Catalytic Reactions						